NJC

Accepted Manuscript

This is an *Accepted Manuscript*, which has been through the Royal Society of Chemistry peer review process and has been accepted for publication.

Accepted Manuscripts are published online shortly after acceptance, before technical editing, formatting and proof reading. Using this free service, authors can make their results available to the community, in citable form, before we publish the edited article. We will replace this *Accepted Manuscript* with the edited and formatted *Advance Article* as soon as it is available.

You can find more information about *Accepted Manuscripts* in the Information for Authors.

Please note that technical editing may introduce minor changes to the text and/or graphics, which may alter content. The journal's standard Terms & Conditions and the Ethical guidelines still apply. In no event shall the Royal Society of Chemistry be held responsible for any errors or omissions in this *Accepted Manuscript* or any consequences arising from the use of any information it contains.

ROYAL SOCIETY OF CHEMISTRY

www.rsc.org/njc

Journal Name

RSCPublishing

ARTICLE

Adsorption and Self-Assembly of a Ferrocene D- and L- Nonapeptide Disulfide onto Gold and Mica Substrates

Cite this: DOI: 10.1039/x0xx00000x

Received 00th January 2012,
Accepted 00th January 2012

DOI: 10.1039/x0xx00000x

www.rsc.org/

V. A. Hernandez Ramirez,[a] A.Pailleret,[b] S.Joiret,[b] F.d'Orlyé,[c-f] M.Lazerges,[*c,f] H.Perrot,[b] S. Gutierrez Granados,[a]F.Bedioui[c-f] and L. M. De León-Rodríguez*[a]

A ferrocene-conjugated nonapeptide composed of alternating D- and L- residues and containing two sulfide linkages was synthesized ($_L$Cys-$_D$Phe-$_L$Phe-$_D$Phe-(Ferrocene)$_L$Lys-$_D$Ala-$_L$Asp-$_D$Ala-$_L$Cys-NH_2) as novel material for nanostructures formation. The cyclic nonapeptide assembly onto gold was highly disordered and included a large dead volume on the gold surface. Also, a large proportion of ferrocene units (79%) were located in microenvironments where electron transfer was hindered. On the other hand, two kinds of self- assembled nanostructure morphologies: linear and rings were observed on mica, depending on the age of the peptide solution used in the adsorption process. Linear nanostructures, 100-1000 nm in length and 1.5-4.0 nm in height, were observed by AFM when using freshly prepared peptide solutions. Rings, 100-200 nm in diameter and 1.6 nm in height were obtained when using a 2-month aged peptide solution.

Introduction

Understanding how short peptides self-assemble into nanostructures is of great interest given their potential application in the design of nano-reactors, biological sensors, electronics, drug delivery systems and stimulus-responsive materials.[1] Several peptide nano-assembly morphologies have been reported in the literature (*e.g.* vesicles, fibers, tubes, tapes and ribbons) and it is known that several factors play a role for obtaining a given architecture with specific physicochemical properties (*e.g.* solvent polarity, ions, peptide concentration, peptide functional groups).[2-4] However, a clear understanding of the mechanisms that generate a particular morphology remains elusive. Studies of peptide self-assembly are carried out not only in solution but also in different solid substrates (*e.g.* mica, gold).[5] These substrates function as templates or supports during the assembling process, as a way to generate nanostructures with specific shape and size[6] and have been used for *in vitro* investigation of diseases related to protein morphology changes, (*e.g.* Alzheimer pathology)[7] or for generating nano-composite materials applied in sensors development for instance. Ferrocene-conjugated peptides (Fc-p's) are an important class of systems widely studied for the development of biological sensors. Excellent reviews of Fc-p's covering topics about their design, synthesis and applications can be found in the literature.[8-11] In general when designing biosensors the peptide sequence of Fc-p's is selected so that it specifically interacts with a target biomolecule (*e.g.* protein) and such interaction is then measured by changes on the electrochemical signal of the ferrocene moiety. To give an idea on recent state of the art on biosensor development with Fc-p's composite materials, one can mention the electrochemical sensor designed for the detection of the aspartic protease encoded by the HIV-1 virus.[12, 13] In this work, perthiolated single walled carbon nanotubes (ptSWCNs) were deposited onto gold electrodes first and then gold nanoparticles (AuNPs) were attached through the ptSWCNs free thiol groups. The AuNPs were then derivatized with a thiolated Fc-pepstatin conjugate, which allowed sensitive and selective detection of the enzyme via the electrochemical response of the ferrocene moiety. This nanostructure integration has attracted much attention given its high surface area, favorable electronic properties and electrocatalytic effects. Although the advantages in the electrochemical properties for such SWCNs composite electrodes are well known, their synthesis and individual component integration might be complex. In this respect biomolecular self- assembly may offer another alternative. Our research group is interested in developing these alternatives and in particular we have focused on the synthesis of cyclic peptide sequences constituted by alternate D and L aminoacids which are known to assemble into nanotube (PNT) like structures.[14-16] The preparation of PNTs composite systems has been well documented in the literature. The first work was reported by Ghadiri*et al.* whom have incorporated an eight-residue cyclic peptide of alternating units of $_D$Leu and $_L$Trp into monolayers

of dodecanethiol and octadecylsulfide formed on gold.[16] The authors observed different structures onto the electrode surface, depending on the experimental conditions used to form the monolayer. Few years later, it was shown that the morphology of D and L cyclic hexapeptide based nanotubes onto gold substrates depends on the aminoacid sequence.[17] For instance, it was reported that a cyclo-hexapeptide with alternating $_D$Cys and $_L$Gln aminoacids forms ring-shaped nanostructures on gold substrates while a random aminoacid sequence containing one $_D$Cys within its structure formed isolated nanotubes. These findings allow one to infer that the presence of three Cys in the cyclic peptide c($_D$Cys-$_L$Gln)$_3$ favors interactions with Au given the possibility to form three strong S-Au bonds. This scenario can explain the fact that the backbone of this cyclopeptide lies parallel to the substrate surface. On the other hand, when only one Cys residue is present; there is only one possible linkage point between the substrate surface and the peptide. This explains the formation of single nanotubes.

As a novel design, in this work we proposed the synthesis of a 9- residues peptide (nonapeptide) containing D and L alternating aminoacids with Cys residues in the N- and C-terminal groups. The peptide sequence is $_L$Cys-$_D$Phe-$_L$Phe-$_D$Phe-(Fc)$_L$Lys-$_D$Ala-$_L$Asp-$_D$Ala-$_L$Cys-NH_2 where a ferrocene (Fc) unit is attached to the middle lysine residue in order to obtain an electroactive material. We hypothesize that the two Cys residues placed at both ends of the nonapeptide will independently bind to a gold substrate and possibly will self-assemble as surface bridged nanotubes given intermolecular hydrogen bond interactions; similar to the ones found for the cyclic peptide derivatives. The peptide is composed mainly of non-polar residues to favor peptide nano-assembly over peptide interactions with polar solvents. A polar Asp residue and an end amino group are also present to confer partial solubility to the peptide. To the best of our knowledge, this kind of designs have not been previously studied, and therefore in this work the self assembly of the ferrocene containing nonapeptide onto gold and mica surfaces was investigated.

Results and Discussion

Peptide Synthesis

The ferrocene labeled nonapeptide (Fc-nonapeptide) was prepared by following standard solid phase peptide synthesis protocols as described in the experimental section. Specific labeling of the peptide with ferrocene was achieved by an orthogonal protection approach. For this, a Lys residue was positioned in the middle of the peptide sequence and the ε-amino group of this Lys was protected with 1-(4,4- dimethyl-2,6-dioxocyclohex-1-ylidene)-3-methylbutyl (ivDde) which is labile to hydrazine. Something to consider under this scheme is that the fluorenylmethyl carbonyl (Fmoc) group is also removed with hydrazine and therefore the end N-aminoacid of the peptide sequence should not be protected with Fmoc but with an acid labile protecting group such as tert-butyloxycarbonyl (Boc). The crude deprotected peptide had to be purified twice by HPLC to remove small amounts of the ferrocene non-labelednonapeptide (MALD-TOF+ m/z 1050.42 (calcld.1050.45) $[M+H]^+$) and an unidentified impurity with m/z 1142.42. The Fc- nonapeptide appeared non-cyclic (MALD-TOF+) m/z 1262.34 (calcld.1262.45) $[M+H]^+$, which agrees with what has been previously reported that disulfide bond formation would be geometrically constraint for D,L cyclic peptides containing an odd number of residues.[18]

Peptide assembly onto gold

We proceeded to study the assembly of the Fc-cyclic-nonapeptide onto gold. The gold substrate used for these experiments was a nanostructured gold pattern (≈ 100 nm thick) deposited onto a 1 cm^2 monocrystalline mica sheet. The gold surface was cleaned by treating it with a 50 μL drop of H_2O_2 30%:H_2SO_4 5% 1:1 v:v for 10 min. A 100 μL drop of a 200 μg/mL peptide CH_3CN:H_2O solution was then deposited onto the gold substrate during different times and SEM images were recorded (Fig. 1). For an adsorption time of 2 min. (Fig. 1B), the gold defects of the gold islands (Fig. 1A) were smoothed, due to deposition of a peptide thin layer below the 1 nm SEM resolution. For a 5 min. adsorption time (Fig 1C), a peptide deposit 8.1 ± 0.1 nm thick was observed at the gold island borders. It is interesting to note that gold islands linked by peptide film domains were also observed (Fig 1C), which suggests a non-homogeneous peptide deposition on the gold surface.

Dynamic growth of peptide films was investigated with a 27 MHz quartz crystal microbalance (QCM). A gold covered quartz was preliminary cleaned with the protocol used for gold covered mica (50 μL drop of H_2O_2 30%:H_2SO_4 95% mixture). The quartz frequency was then monitored during successive circulation of H_2O, CH_3CN:H_2O mixture, 200 μg/mL peptide solution in CH_3CN:H_2O mixture and CH_3CN:H_2O mixture again (Fig. 2). The first frequency decrease was attributed to a change of solvent properties, from H_2O to H_2O:CH_3CN mixture. The second frequency change was attributed to peptide self-assembly. The total frequency, $\Delta f(Hz)$, due to film growth was equal to -389 Hz. According to equation [1], for thin layers the mass of the film deposited, $\Delta m(g)$ is proportional to the quartz frequency change multiplied by the sensibility, a, of the QCM (350 pg/Hz).

$$\Delta m = a \times \Delta f \quad [1]$$

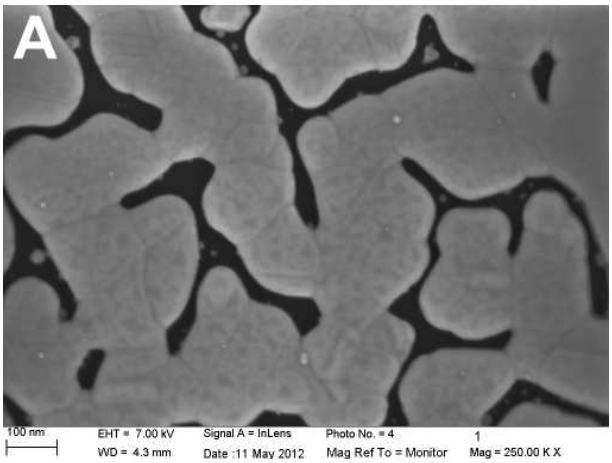

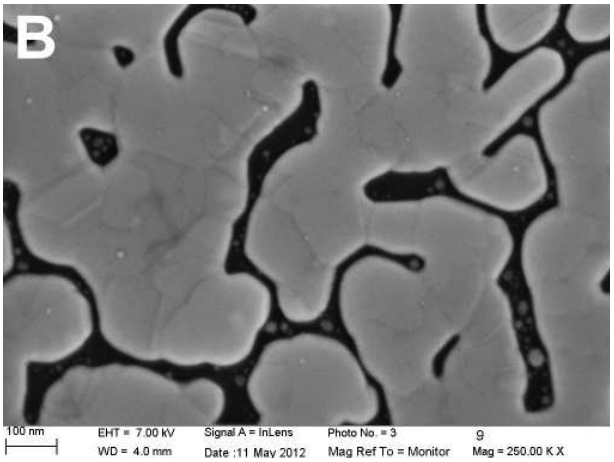

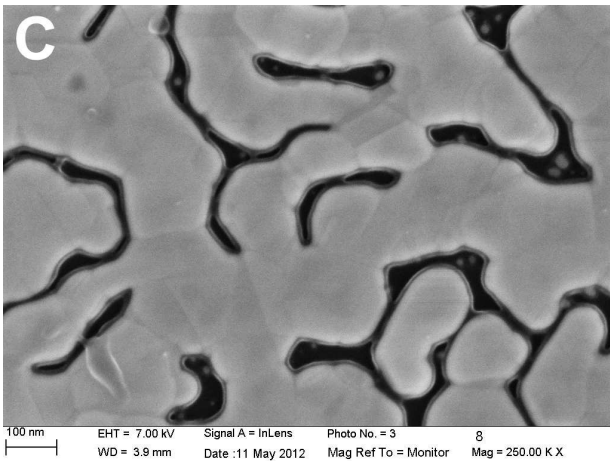

Fig. 1 Sweep electron microscopy analysis of gold substrate (A) and peptide films formed on a 1 cm^2 gold substrate by adsorption of a 100 μL drop of 200 μg/mL peptide $CH_3CN:H_2O$ solution for 2 min. (B) and 5 min. (C).

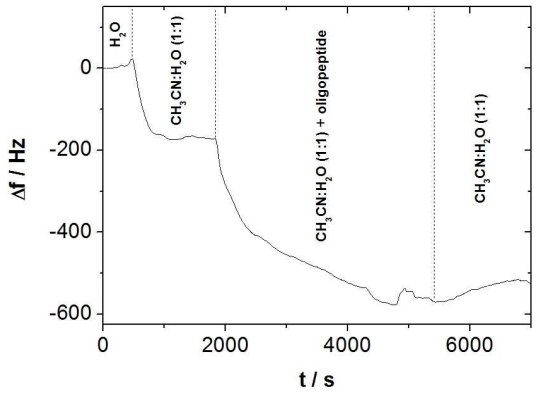

Fig. 2 Quartz crystal microbalance frequency monitoring of peptide filmgrowth onto gold substrate: successive circulation of H_2O, $CH_3CN:H_2O$mixture, 200 μg/mL peptide solution in $CH_3CN:H_2O$ solution and$CH_3CN:H_2O$ mixture.

Thus the calculated amount of peptide for a 5 min. deposition time was 56.0 ng, which corresponds to a - 159 Hz frequency change. 56.0 ng have an effective surface coverage (Γ) of 5.6 × 10^{-10} mol.cm^{-2} or 3.4 × 10^{14} molecules.cm^{-2} which corresponds to an effective particle area of 3.0 nm^2. This value is comparable to the average face surface area of a rectangular prism enclosing an optimized peptide structure in a β-helix (2.8 nm^2) or a U-shaped (3.2 nm^2) conformation (2.6 nm^2 for β-sheet) (Fig. 3), which are the ones commonly observed for D,L-alternating peptides.[19-21]

The peptide film density was estimated using equation [2]:

$$d = m / h.A.\rho H_2O \quad [2]$$

Where m is the film mass obtained from the QCM run (56.0 ng), h is the film thickness estimated by SEM (8.1 nm), A is the gold covered quartz area (0.196 cm^2) and ρH_2O is the water volumic mass (1 g/cm^3). It is important to mention that the h value measured by SEM might not be equal to the value expected under QCM conditions since the former are performed under vacuum and the later are performed in aqueous media.

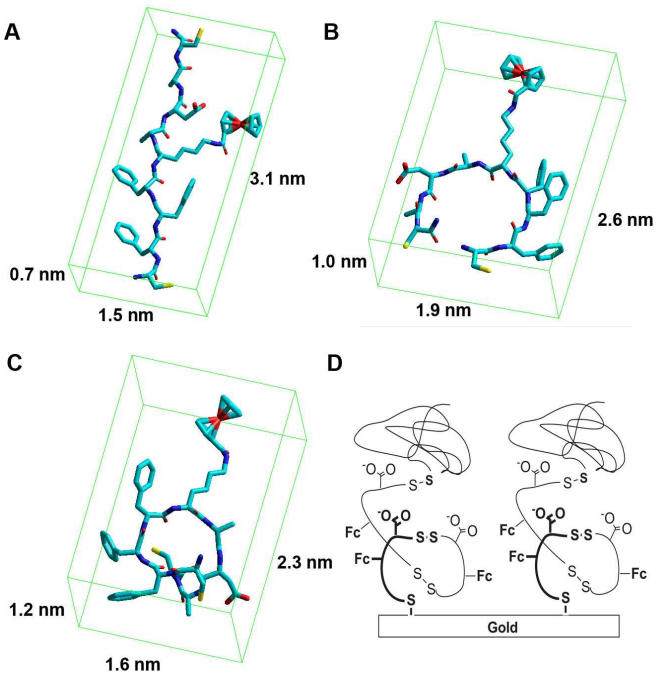

Fig. 3 HyperChem molecular model for the Fc- nonapeptide in a A) β-sheet, B) U-shaped and C) β-helix conformation. The peptide is shown in tube rendering where light blue color corresponds to carbon, dark blue to nitrogen, red to oxygen and yellow to sulfur atoms. For clarity purposes hydrogen atoms are omitted. D) Model of peptide deposition on gold.

Therefore, the density determined herein would be larger than the expected value in solution, where the *h* value will be larger due to solvation effects. The calculated density *d* value was 0.35, which is close to 20% of the density of a crystallized peptide (*d* = 1.5), meaning that the peptide film assembly on gold include a large dead volume and is more likely highly disordered. It is well established that thiol containing compounds chemically adsorb on gold via the covalent S-Au bond. The di-Cys peptide presented herein is mainly hydrophobic but includes an Asp which is hydrophilic. Thus one can depict that the Fc-nonapeptide will form a S-Au bond, with the most hydrophobic side of the peptide (N-end) attached to the surface while keeping the polar residue exposed to the solvent. Intermolecular interactions of the Au-bonded peptide with peptides in solution will arrange to minimize the exposure of the hydrophobic residues of the peptide (including the Fc) to the solvent which can lead to polymerization through disulfide bonds (Fig. 3D).[22] This model explains the growth of the peptide layer up 8.1 nm and gold island linkage by peptide after 5 min deposition observed in SEM as well as the poor density of peptide attached to the surface. Next, we studied the electrochemical response of peptide modified gold electrodes. For these studies an electroactive layer was prepared by immersion of a gold electrode in a 200 µg/mL peptide solution in CH_3CN:H_2O during two hours (Fig. 4). A linear response of the oxidation peak current *Ipeak* with sweep rate *v* ($mV.s^{-1}$) was observed (insert in Fig. 4), which is characteristic of a thin layer (*i.e.* no diffusing limiting step). The peak current in such thin layer response is given by equation [3]:

$$Ipeak = z^2.n.F^2.A.v / 4.R.T \quad [3]$$

Where *z*, equal to 1, is the number of redox electrons for Fc, *n* (mol) is the number of electroactive peptide units into the peptide layer, *F* (96485 $C.mol^{-1}$) is the Faraday constant, *A* the gold area (0.196 cm^2), *v* ($V.s^{-1}$) is the cyclic voltammetry sweep rate, R (8.31 $J.K^{-1}.mol^{-1}$) is the ideal gas constant and *T* (K) is the temperature. The number *n* (mol) of electroactive peptides, calculated using equation [3], was 2.3×10^{-11}mol ($\Gamma = 1.2 \times 10^{-10}$ $mol.cm^{-2}$). The total number of peptide units of the film (calculated by taking into account the -389 Hz frequency shift measured with the QCM during formation of the film using equation [1]) was 1.1×10^{-10} mol. The ratio between electroactive and total peptide units in the film is equal to 0.21, indicating that a large proportion of ferrocene electroactive units (79%) are located in microenvironments where electron transfer is hindered. This can be attributed to enclosure of ferrocene units in peptide hydrophobic pockets (Fig 3D) which in turn hinders penetration of electrolyte ion for charge compensation.[23] The peptide chain is not a molecular conductor (i.e. no π orbitals alternated chain). The ferrocene redox probe is then diluted in an insulating peptide matrix. The polymer thickness (8 nm) is larger than the hopping electronic distance (2 nm), therefore, the electroactive response is limited by hopping, yielding a decrease of current and potential peak shift as shown in the voltammograms of Fig. 4. Given the disordered nature of peptide deposition on gold we proceeded to study peptide deposition on a substrate where no covalent interactions

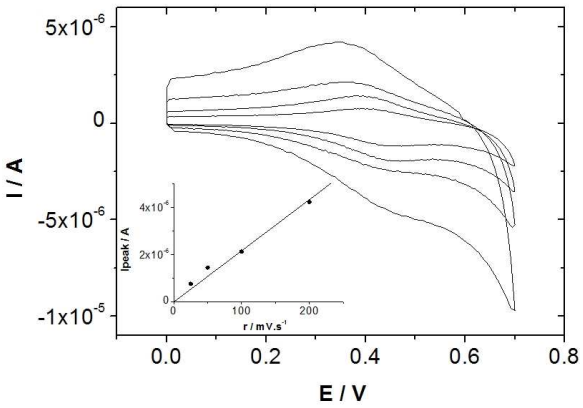

are expected.

Fig. 4 Cyclic voltammetry of peptide at 25, 50, 100 and 200 $mV.s^{-1}$ sweeprates.

Peptide assembly onto mica.

Peptide adsorption was investigated onto potassium aluminosilicate (muscovite mica) surfaces. This surface was chosen because it is a perfectly flat substrate well suited to study isolated single nanostructure formation. A 200 µg/mL fresh peptide solution CH_3CN:H_2O was prepared and a 50 µl drop of this solution was then deposited onto a freshly cleaved 1 cm^2 mica sheet. The solution was removed after 10 min., and the surface was gently cleaned with 2 mL of CH_3CN:H_2O mixture and dried with CO_2. AFM analysis of the substrate

showed bundles of linear nanostructures with 100 to 1000 nm lengths (359.3 ± 153.0 nm (N = 23)) in both topology (Fig. 5A) and phase (Fig. 5B) images. No covalent interaction can be established between the mica substrate and the peptide. Peptides were adsorbed onto the substrate *via* a classic pathway involving non specific interactions (*i.e.* physical adsorption). These nanostructures were observed more clearly when the adsorption time was decreased to 1 min. (Fig. 5C topology, Fig. 5D phase). Under these conditions the linear nanostructures' lengths were as indicated above and the heights for 22 of these nanostructures were 1.4 ± 0.2 nm (N = 6), 1.5 ± 0.2 (N = 2), 2.7 ± 0.2 (N = 10) and 4.0 ± 0.3 nm (N = 4). The height values are comparable to the length of the sides of a rectangular prism enclosing an optimized structure of the Fc-nonapeptide in different conformations (Fig. 3). This suggests that single Fc-nonapeptide units self-assemble to form the linear nanostructures resting on the mica's surface. The larger height (4.0 nm) could be attributed to stacking of two nanostructures possibly due to aromatic interactions. Nanotube formation from cyclic peptides containing alternating L and D aminoacids is due to hydrogen bonding between the carbonyl groups of one cycle and the -NH- amide groups of another cycle, these amide functionalities are almost perpendicular to he tplanar antiparallel cyclic backbones.[14] This kind of arrangement can only be attained if the peptide presented herein adopts a U-shaped conformation, which is in agreement with the experimental data presented in this work. The association constant K of these nanostructures was estimated by following their assembly onto a mica surface at various peptide concentrations. A 50 μg/mL solubility constant at room temperature (23 °C) was measured since nanostructures formation were not observed at lower concentrations. This

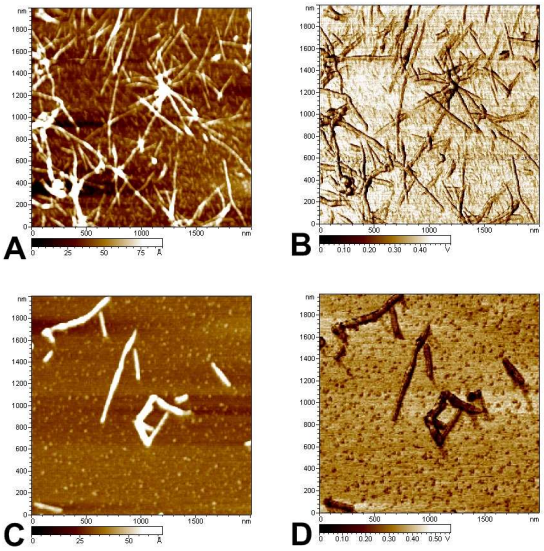

corresponds to a 2.5 × 10^6 M^{-1} association constant K. The 200 μg/mL peptide solution was kept in a fridge at 4 °C during 2 months, and AFM analysis of peptide deposited onto mica using these aged solution was then performed under similar experimental conditions as stated above (*i.e.* 200 μg/mL peptide solution, 10 min.). This time, both curved and ring nanostructures were observed (Fig. 6A and 6C topology, Fig. 6B and 6D phase).

Fig. 5 AFM imaging of peptide nanostructures onto mica sheet surfacesadsorbed from 200 μg/mL freshly prepared peptide solutions inCH_3CN:H_2O, for 10 min. (A topology, B phase) and 1 min. (C topology,D phase) adsorption times.

The ring external diameters varied from 100 to 200 nm (117.3 ± 8.1 nm) and the height was 1.6 ± 0.2 nm (N = 6). With the diameter data one can calculate the perimeter of the ring being equal to 368.3 nm which is similar to the average length of the linear nanostructures (359.3 nm) observed in Fig. 5. This suggests that rings are formed from the linear structures. The phase images of the linear nanostructures prepared from fresh peptide solutions (Fig. 5A and 5C) had a more pronounced contrast than the corresponding topology images (Fig. 5B and 5D). This indicates a crystalline molecular arrangement for the linear assembly, which is in agreement with what has been reported in the literature for other peptide nanostructures.[24] An important question to address was: why are ring nanostructures formed with aged peptide solutions? To answer this question, first we determined if the peptide in aged solutions remained intact. Thus, we obtained HPLC spectra of the peptide's solution at different times during which no change on the chromatographic profile was observed. Therefore, since the peptide remained unchanged when comparing fresh and aged solutions and the conditions for peptide adsorption onto mica were the same for the fresh and aged peptide solution, we concluded that peptide assembly into different morphologies occurred in solution. A similar behaviour has been previously reported for similar self-assembled oligopeptidesystem.[25] Thus, one can infer that the linear nanostructures transition into curve ones first and from these the ring shaped nanotructures are formed.

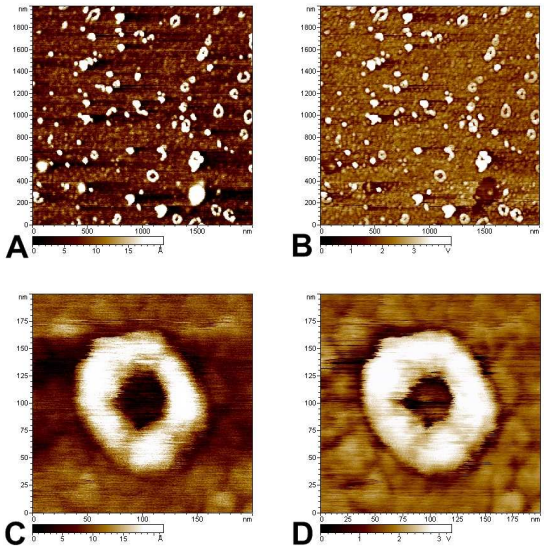

Fig. 6 AFM imaging of peptide nanostructures onto mica sheet surfaces adsorbed from 200 μg/mL aged peptide solutions in $CH_3CN:H_2O$, for a 10 min. (A, C topology - B, D phase) adsorption time.

This was further supported by the observation of some curved nanostructures after treating the mica surface with fresh peptide solution and also that both ring and linear curved nanostructures of similar heights are observed (1.6 and 1.4 nm respectively). A mechanism consistent with experimental observations, is proposed in fig. 7: (i) linear and curved peptide nanostructures are formed (both in equilibrium, (ii)) resulting from the self-assembly of single peptide units; concomitantly, crystalline rods are formed (Fig. 5) as a result of inter tube stacking *via* π-π interactions.

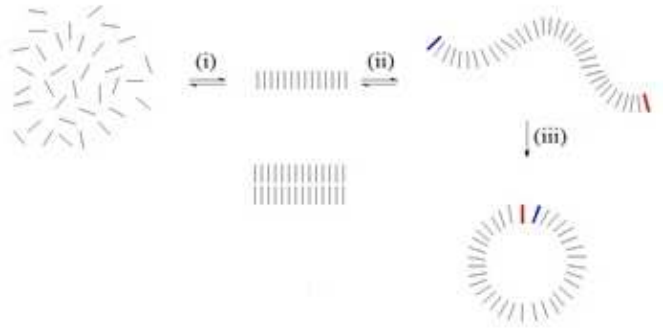

Fig. 7 Self-assembly formation mechanism of (i) linear curved nanostructures, (ii) rod like nanostructures and (iii) circled nanostructures.

(iii) Ring nanostructures that are formed from aged peptide solutions (Fig. 6) result from self-association of terminal peptides in a curved nanostructure. This last hypothesis is consistent with a slow kinetics, as the probability of collision between the two terminal peptide of a 359 nm average lentgh is feeble, and it is also consistent with reversibility between linear and curved nanostructures and the absence of linear nanostructures on mica when using aged peptide solutions.

Experimental section

Materials

Fmoc-Cys(Trt)-OH, Fmoc-DAla-OH, Fmoc-Lys(ivDde)-OH, Fmoc- DPhe-OH, Boc-Cys(Trt)-OH and Rink Amide Novagel were purchased from Novabiochem. Fmoc-Asp(tBu)-OH and Fmoc-Phe-OH were obtained from SynPep Corp. 1-Hydroxybenzotriazole (HOBt), 2-(1H-Benzotriazole-1-yl)-1,1,3,3-tetramethyluroniumhexafluorophosphate (HBTU), N,N-Diisopropylethylamine (DIPEA), hydrazine, ferrocenecarboxylic acid (Fc-COOH), triisopropylsilane (TIPS), trifluoroacetic acid (TFA) and diethyl ether anhydrous were purchased from Aldrich. Solvents were obtained from Fisher Scientific. Water was obtained from a Milli-Q systemem (Millipore Inc.) and had a resistivity of 18.2 MΩ. All chemical reagents were of analytical grade and were used without further purification.

Equipment and Methods

Analytical HPLC was performed on a Agilent 1200 system using a Jupiter 5μ C18 300Å, 250 mm ×4.6 mm column from Phenomenex with a flow rate of 1 mL/min. SemipreparativeHPLC was performed using Jupiter 10μC18 300Å, 250 mm ×10 mm column from Phenomenex with a flow rate of 4.73 mL/min. Solvent A was water, solvent B was acetonitrile and both solvents include 0.1% trifluoroacetic acid.
MALDI-TOF (matrix-assisted laser desorption/ionization time-of-flight) mass spectra were measured with a Voyager-DE PRO BiospectrometryWorkstation from Applied Biosystems operating in reflector positive mode and using α-cyano-4-hydroxycinnamic acid as the matrix.
Raman analysis was carried out in a Raman spectrometer equipment consisting of a microscope (Olympus BX40) coupled to a 300 mm focal length spectrograph from HORIBA JobinYvonLABRAM equipped with a 1800 grooves / mm holographic grating and a 1024 ×256 pixels Peltier air cooled CCD detector. The spectra are obtained with 632.817 nm radiation from an internal 10 mW He-Ne laser. An ULWD (ultra-long working distance) objective allows to record Raman spectra with a working distance of 8 mm. Confocal hole was set at 200 μm. Spectrum was recorded from 250 to 3100 cm^{-1}.
1H-NMR spectra were recorded on a Varian Gemini: Unity plus 200 MHz. Spectra was collected in a mixture of $D_2O/CD_3CN/H_2O$. Data reported the chemical shifts in ppm(δ).
AFM observations were carried out in air using a Molecular Imaging instrument in the acoustic resonant mode. This was composed of a Pico-LE base equipped with a micropositioning device aimed at the precise positioning of the AFM tip in the x-y plane of the sample, a 100 μm x 100 μm large zone scanner bearing a photodetector and the AFM nose adequate for TM-AFM experiments. A PicoScan 2100 controller connected to a computer was used to drive the scanner and to collect the data generated by the laser impact on the photo detector. For this purpose, rectangular silicon cantilevers bearing conical silicon tips were used. Their resonance frequency was 280-365 kHz, and their spring constant was 25-50 $N.m^{-1}$. All AFM images shown hereafter underwent a plane correction process.
Scanning Electronic Microscopy (SEM) was performed with a 70 high-resolution Ultra 55 Zeiss.
The resonator of the quartz crystal microbalance (QCM) was a Matel-Fordhal France AT-cut planar quartz crystal, 14 mm-diameter, with a 9 MHz nominal resonance frequency. Two 5 mm-diameter identical gold electrodes, 200 nm-thick, were deposited by evaporation techniques on both sides of piezoelectric quartz, with a 25 nm chromium under-layer. The resonator was connected by a silver conducting paste, through wires, to a BNC connector. A home-made oscillator was designed to drive the crystal at 27 MHz, which corresponds to the third over tone of the 9 MHz quartz resonator. To improve the stability, all the electronic oscillator components were

temperature- controlled by a Watlow heater monitor with stability better than 0.1 °C. The crystal was mounted between two O-ring seals inserted in a home- made plexiglass cell. Only one face of the quartz was in contact with the solutions. The cell volume was 50 µL. The apparatus includes a Pharmacia micropump to assure a 50 µL/min constant flow of the solutions in the quartz cell. The frequency was measured with a PM 6685 frequency counter and recorded with a home-made C language.

The electrochemical experiments were performed using a PG580Potentiostat/Galvanostat (Princeton Applied Research). The cyclic voltammetry runs were performed in deoxygenated aqueous solutions, by previously bubbling pure argon gas for 10 min., in a 10 mL electrochemical cell with a Pt counter electrode, a Ag/AgCl/3M NaCl reference electrode and a 5 mm diameter quartz crystal resonator metallized with a gold layer as a work electrode. Gold surface was cleaned with a H_2SO_4:H_2O_2 30% v:v 1:1 mixture during 20 min., and rinsed with deionized water. Self-assembled monolayers of the peptide were prepared by deposition of 150 µL drop of 200 µg/mL peptide solution in CH_3CN:H_2O 1:1 v:v during 1 h. and gold surface was then rinsed with deionized water. Voltammograms of modified electrodes were recorded in a 0.1 M phosphate buffer solution pH 7.4.

Peptide Synthesis, Purification and Characterization

The nonapeptidelabeled with ferrocene was synthesized by solid phase peptide synthesis using the Fmoc protocol: $_L$Cys-$_D$Phe-$_L$Phe-$_D$Phe-(Fc)$_L$Lys-$_D$Ala-$_L$Asp-$_D$Ala-$_L$Cys-NH_2 (scheme 1). The Fmoc protecting group was removed by gently shaking the resin with a 20% solution of piperidine in DMF for 2 hours. Amino acids were attached to the Rink Amide Novagel resin by using single-step couplings of 3 equiv. of Fmoc-amino acid, 2.9 equiv. HBTU and HOBt, and 6 equiv. DIPEA in DMF in the order Fmoc-Cys(Trt)-OH, Fmoc-$_D$Ala-OH, Fmoc-Asp(tBu)-OH, Fmoc-$_D$Ala-OH, Fmoc-$_L$Lys(ivDde)-OH, Fmoc-$_D$Phe-OH, Fmoc-$_L$Phe- OH, Fmoc-$_D$Phe-OH and Boc-$_L$Cys(Trt)-OH. After the last aminoacid was coupled the ivDde protecting group was selectively removed by treating the resin with a solution of 2% hydrazine in DMF for 2 hours. The protected peptide attached to the resin was labeled with ferrocene by coupling ferrocenecarboxylic acid to the ε-amino group of the lysine residue using the same coupling conditions as described for the protected amino acids. The peptide was removed from the resin and protecting groups were cleaved from the peptide by treating the resin with a mixture of TFA/H_2O/TIPS (95/2.5/2.5) for 2 hours. The resin was filtered out and then washed with fresh TFA. The combined filtrates were collected and solvent removed under a gentle nitrogen flow. Crude peptide was precipitated with cold ether and the solid obtained was decanted. Crude product was purified twice by HPLC and the fractions containing the desired product were freeze dried giving a yellow powder with an overall yield of 16.7%. Product was characterized by MS (MALDI-TOF+), Raman spectroscopy and ^{1}H NMR (see ESI). (MALDI-TOF+) *m/z* = 1262.34 (100%) (calcld. 1262.45) $[M+H]^+$, 1263.37 (74%), 1264.41 (30%), 1284.38 [M+Na]+; 1HNMR (200 MHz, D_2O/CD_3CN): δ 8.9-8.5, 8.0-7.5, 5.4-5.0, 4.3 (Fc), 3.8, 3.7-3.2, 2.6, 2.4-2.0, 1.7. Raman spectroscopy: C-C ring (Fc cyclopentadienyl) 999.4 cm^{-1}, C-C ring (phenylalanine) 1027.9 cm^{-1}, 1100.0 cm^{-1}. The peptide solutions used in the AFM, SEM and QCM experiments were prepared with a 1:1 (v:v) mixture of CH_3CN:H_2O and the experiments were performed at 23 ± 2 °C.

Computational Studies

Peptide's structures were built and optimized using HyperChem™ 7.52 from Hypercube. The β sheet and β helix conformations of the peptide were constructed from the aminoacids data base of Hyperchem and the U-shaped conformation was built using Φ_L = -139 °, Ψ_L = 160 °, Φ_D = 139° and Ψ_D = -160° dihedral angles, which are the optimum reported values for a 10 residue L-, D- cyclic peptide.[26] Peptide's geometry optimization was done without the ferrocene units using the Molecular Mechanics force field BIO+(CHARMM) using the Polak-Ribiere algorithm until the termination condition of 0.01 Kcal/(Å.mol) RMS gradient was met. Pre-optimized ferrocenecarboxyl units were manually bonded to the corresponding lysine residue of the optimized peptide structure and optimization of the Ferrocene carboxylamide unit was carried out while maintaining the rest of the structure fixed.

Conclusions

A ferrocene labeled nonapeptide conformed of alternating D and L aminoacids was successfully synthesized. This peptide showed a disordered assembling process on gold. When adsorbed on mica, the peptide presented a unique morphological dynamic transition from linear to ring shaped nanostructures. A mechanism describing this transition is proposed. Such approach is a useful tool to tailor specific nanostructure shapes.

Acknowledgements

We wish to thank Stephan Borensztajn for scanning electron microscopy analysis of peptide thin films.

Notes and references

[a] *Universidad de Guanajuato, Departamento de Química, Cerro de la Venada S/N, Pueblito de Rocha, 36040, Guanajuato, Gto, México. Fax/Tel:524737326252;E-mail:lmdeleon@ugto.mx*

[b] *Université Pierre et Marie Curie, LISE, UPR 15 CNRS, 4 Place Jussieu, 75005 Paris, France*

[c] *Chimie ParisTech, Ecole Nationale Supérieure De Chimie De Paris, Unité de Technologies Chimiques et Biologiques pour la Santé, Paris, France*

[d] *CNRS, Unité de Technologies Chimiques et Biologiques pour la Santé, UMR 8258, Paris, France*

[e] *Université Paris Descartes, Sorbonne Paris Cité, Unité de Technologies Chimiques et Biologiques pour la Santé, Paris, France*

[f]INSERM, Unité de Technologies Chimiques et Biologiques pour la Santé (N ◦ 1022), Paris, France; Fax: 33144276496;Tel.:33144276497;Email:mathieu.lazerges@parisdescartes.fr

1. A. B. Seabra and N. Durán, *Peptides*, 2013, **39**, 47-54.
2. Q. Meng, Y. Kou, X. Ma, Y. Liang, L. Guo, C. Ni and K. Liu, *Langmuir*, 2012, **28**, 5017-5022.
3. H. Xu, J. Wang, S. Han, D. Yu, H. Zhang, D. Xia, X. Zhao, T. A.Waigh and J. R. Lu, *Langmuir*, 2009, **25**, 4115-4123.
4. H. Yang, M. Pritzker, S. Y. Fung, Y. Sheng, W. Wang and P. Chen, *Langmuir*, 2006, **22**, 8553-8562.
5. C. Whitehouse, J. Fang, A. Aggeli, M. Bell, R. Brydson, C. W. G. Fishwick, J. R. Henderson, C. M. Knobler, R. W. Owens, N. H. Thomson, D. A. Smith and N. Boden, *Angew. Chem. Int. Edit.*, 2005, **44**, 1965-1968.
6. F.Zhang, H.N.Du, Z.X.Zhang, L.N.Ji, H.T.Li, L.Tang, H.B. Wang, C. H. Fan, H. J. Xu, Y. Zhang, J. Hu, H. Y. Hu and J. H. He, *Angew. Chem. Int. Edit.*, 2006, **45**, 3611-3613.
7. U. Anand and M. Mukherjee, *Langmuir*, 2013, **29**, 2713-2721.
8. S. Martić, M. Labib, P. O. Shipman and H. B. Kraatz, *Dalton T.*, 2011, **40**, 7264-7290.
9. A. Lataifeh, S. Beheshti and H. B. Kraatz, Eur. *J. Inorg. Chem.*, 2009, 3205-3218.
10. H. B. Kraatz, *J. Inorg. Organomet. P.*, 2005, **15**, 83-106.
11. T. Moriuchi and T. Hirao, *Acc. Chem. Res.*, 2010, **43**, 1040-1051.
12. K. A. Mahmoud, S. Hrapovic and J. H. T. Luong, *ACS Nano*, 2008, **2**, 1051-1057.
13. K. A. Mahmoud and J. H. T. Luong, *Anal. Chem.*, 2008, **80**, 7056-7062.
14. M. R. Ghadiri, J. R. Granja, R. A. Milligan, D. E. McRee and N. Khazanovich, *Nature*, 1993, **366**, 324-327.
15. D. T. Bong, T. D. Clark, J. R. Granja and M. R. Ghadiri, *Angew. Chem. Int. Ed. Engl.*, 2001, **40**, 988-1011.
16. K. Motesharei and M. R. Ghadiri, *J. Am. Chem. Soc.,* 1997, **119**, 11306-11312.
17. H. Okamoto, T. Yamada, H. Miyazaki, T. Nakanishi, K. Takeda, K. Usui, I. Obataya, H. Mhara, H. Azehara, W. Mizutani, K. Hashimoto, H. Yamaguchi and Y. Hirayama, *Jpn. J. Appl. Phys. 1*, 2005, **44**, 8240-8248.
18. A. Ortiz-Acevedo and G. R. Dieckmann, *Tetrahedron Lett.*, 2004, **45**, 6795-6798.
19. A. Küsel, Z. Khattari, P. E. Schneggenburger, A. Banerjee, T. Salditt and U. Diederichsen, *ChemPhysChem*, 2007, **8**, 2336-2343.
20. E. Navarro, E. Fenude and B. Celda, *Biopolymers*, 2004, **73**, 229-241.
21. B. Di Blasio, V. Del Duca, A. Lombardi, C. Pedone, G. P. Lorenziz and E. Benedetti, *Int. J. Pept. Prot. Res.*, 1995, **45**, 100-105.
22 M. Lazerges, H. Perrot, N. Rabehagasoa, E. Antoine, C. Compere, *Chem.Commun.*, 2005, 6020-6022.
23. S. Chen, *Langmuir*, 2001, **17**, 6664-6668.
24. R. Stiufiuc, F. Toderas, M. Iosin and G. Stiufiuc, *Int. J. Mod. Phys. B*, 2010, **24**, 757-761.
25. V. Haridas, S. Sahu and A. R. Sapala, *Chem. Comm.*, 2012, **48**, 3821-3823.
26. H. Okamoto, T. Nakanishi, Y. Nagai, M. Kasahara and K. Takeda, *J. Am. Chem. Soc.*, 2003, **125**, 2756-2769.

Inserting Graphics

Graphics should be inserted where they are first mentioned (unless they are equations, which appear in the flow of the text). They can be single column or double column as appropriate.

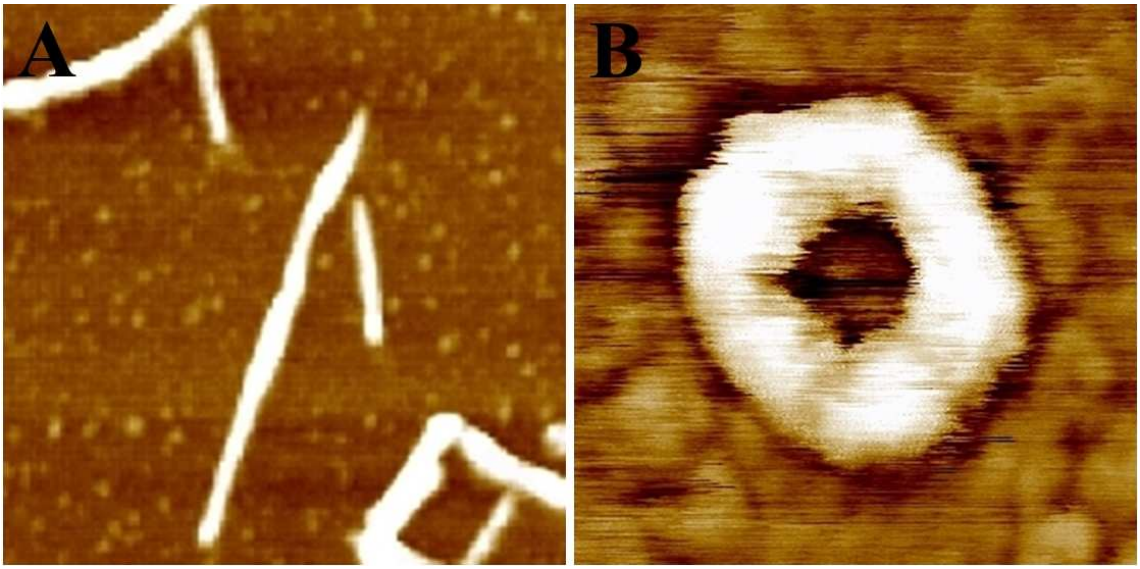

Linear nanostrucutures resulting form self-association of a nonapeptide (A) yield progressively to ring-shaped nanostructures (B).